Gibberellins accumulate in the elongating endodermal cells of *Arabidopsis* root

Eilon Shani[a,1], Roy Weinstain[b,1], Yi Zhang[a], Cristina Castillejo[a], Eirini Kaiserli[c], Joanne Chory[c,d], Roger Y. Tsien[b,e,f], and Mark Estelle[a,f,2]

[a]Section of Cell and Developmental Biology, Departments of [b]Pharmacology and [e]Chemistry and Biochemistry, and [f]Howard Hughes Medical Institute, University of California at San Diego, La Jolla, CA 92093; and [c]Plant Biology Laboratory, and [d]Howard Hughes Medical Institute, The Salk Institute for Biological Studies, La Jolla, CA 92037

Contributed by Mark Estelle, January 10, 2013 (sent for review November 12, 2012)

Plant hormones are small-molecule signaling compounds that are collectively involved in all aspects of plant growth and development. Unlike animals, plants actively regulate the spatial distribution of several of their hormones. For example, auxin transport results in the formation of auxin maxima that have a key role in developmental patterning. However, the spatial distribution of the other plant hormones, including gibberellic acid (GA), is largely unknown. To address this, we generated two bioactive fluorescent GA compounds and studied their distribution in *Arabidopsis thaliana* roots. The labeled GAs specifically accumulated in the endodermal cells of the root elongation zone. Pharmacological studies, along with examination of mutants affected in endodermal specification, indicate that GA accumulation is an active and highly regulated process. Our results strongly suggest the presence of an active GA transport mechanism that would represent an additional level of GA regulation.

root development | ethylene | root growth | fluorescent labeling | hormone labeling

Adaptive growth of plants is regulated by small-molecule regulators called plant hormones (1). Plants regulate hormone response pathways at multiple levels including hormone biosynthesis, metabolism, perception, and signaling. In the case of auxin, elegant studies have shown that the regulation of auxin distribution through the action of specific transporters also has a central role in plant development (2, 3). The recent isolation of transporters for other hormones (4–6) suggests that the spatial distribution of these compounds may also be regulated.

Gibberellins (GAs) are a class of tetracyclic diterpenoid hormones that regulate many developmental processes such as seed germination, root and shoot elongation, flowering and fruit patterning (7–9). Over the years, more than 130 GAs have been identified, of which only a few, such as GA_1, GA_3, and GA_4, are bioactive (8). Much progress has been made in understanding how plants control GA response through regulation of biosynthesis, metabolism, and signaling (10–14). Although experiments with radiolabeled GAs as well as grafting studies have established that GAs move through the plant (15–18), little is known about either the mechanisms of transport or the distribution of GA.

To address these questions, we generated fluorescently tagged GA. The labeled GAs retained much of their bioactivity and thus were used as fluorescent GA surrogates to study the distribution of GA in the *Arabidopsis* root system.

Results

Fluorescently Labeled GAs Are Bioactive. Four derivatives of fluorescein (Fl)-labeled GA_3 were synthesized (*SI Appendix*, Figs. S1–S4), varying primarily in the length of the linker between Fl and GA_3 (Fig. 1*A* and *SI Appendix*, Fig. S5*A*). Conjugation to GA_3 through amide formation on C6 was based on previous reports demonstrating its stability in vitro and in vivo (19). The four molecules were compared for their GA bioactivity. GAs are essential for seed germination in many plants including *Arabidopsis* (20, 21). The GA biosynthesis mutant *ga1* germinates poorly, whereas exogenous application of GA_3 fully restores germination levels (22, 23). Whereas molecules **1** and **4** had a very small effect on *ga1* germination (4% and 8%, respectively), treatment with molecules **2** and **3** resulted in 33% and 53% germination. Application of Fl to *ga1* plants had no effect on germination (Fig. 1*B* and *SI Appendix*, Fig. S5*B*). Similarly, for wild-type (WT) plants treated with the GA-biosynthesis inhibitor paclobutrazol (Paclo), molecules **2** and **3** showed the highest rate of germination (38% and 27%, respectively), whereas **1** and **4** had a smaller effect (13% and 16%, respectively) and Fl had no effect at all (*SI Appendix*, Fig. S5*C*). GAs are also key regulators of hypocotyl and root elongation (24, 25). In 4-d-old WT seedlings treated with Paclo, molecules **1**, **4**, and Fl had little effect on Paclo-treated hypocotyls whereas **2** and **3** partially restored elongation (73% and 69%, respectively) (Fig. 1 *C* and *D* and *SI Appendix*, Fig. S5 *D* and *E*). Strikingly, in WT plants treated with Paclo, application of molecules **2** and **3** fully restored root elongation, compared with GA_3, whereas **1** and **4** had only a modest effect (Fig. 1*E* and *SI Appendix*, Fig. S5*F*). In this assay, the half-maximal effective concentration (EC_{50}) of the best performing derivative molecule **3** (termed "GA_3-Fl" from here on) was 130% that of GA_3 (1.13 ± 0.02 μM and 0.87 ± 0.11 μM, respectively) (Fig. 1*F*). Together, these results demonstrate that GA_3 can be labeled with fluorescein and retain biological activity. Structurally, there is a positive correlation between linker length and bioactivity. Reintroduction of the carboxylic acid in close proximity to its original location on GA's C6 (molecule **4**) did not have a positive effect on bioactivity. To further evaluate tagged GA function across species, we tested GA_3-Fl bioactivity in *Solanum lycopersicum* (tomato) compound leaf development. Tomato plants treated with GA_3-Fl presented simpler leaves with smooth margins, mimicking GA's effect on tomato leaf shape (*SI Appendix*, Fig. S6).

The minor structural differences between GAs prompted us to test whether the strategy used for GA_3 labeling is also effective for other bioactive GAs. Thus, GA_4 was labeled with fluorescein similarly to GA_3-Fl (Fig. 1*G*) and tested for its activity. The fluorescent conjugate (GA_4-Fl) had comparable activity to GA_4 with respect to germination (Fig. 1*H*) and root and hypocotyl elongation (*SI Appendix*, Fig. S7). This suggests that the GA-labeling strategy described here could be applied to other GA derivatives. GA_3-Fl and GA_4-Fl have spectroscopic properties characteristic of fluorescein (λ_{ex} = 496 nm, λ_{em} = 523 nm, Φ_f = 0.81 and λ_{ex} = 495 nm, λ_{em} = 525 nm, Φ_f = 0.75, respectively) (*SI Appendix*, Fig. S8), making them suitable for detection by fluorescence imaging.

Author contributions: E.S., R.W., Y.Z., R.Y.T., and M.E. designed research; E.S., R.W., and Y.Z. performed research; C.C., E.K., and J.C. contributed new reagents/analytic tools; E.S., R.W., Y.Z., R.Y.T., and M.E. analyzed data; and E.S., R.W., R.Y.T., and M.E. wrote the paper.

The authors declare no conflict of interest.

See Commentary on page 4443.

[1]E.S. and R.W. contributed equally to this work.

[2]To whom correspondence should be addressed. E-mail: mestelle@ucsd.edu.

This article contains supporting information online at www.pnas.org/lookup/suppl/doi:10.1073/pnas.1300436110/-/DCSupplemental.

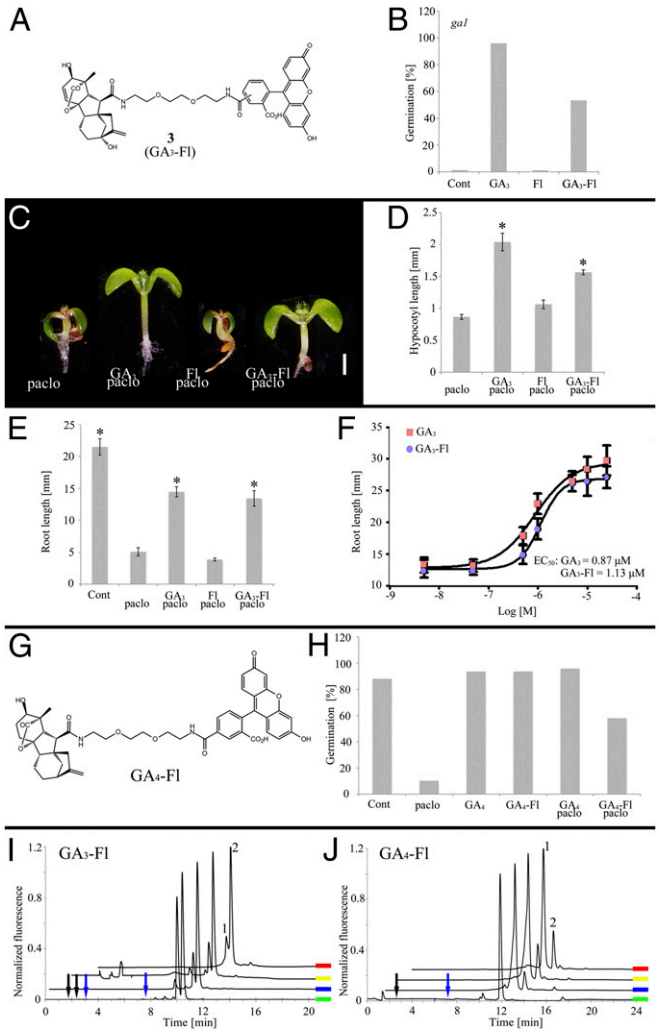

Fig. 1. Characterization of labeled GAs. (*A*) Molecular structure of GA_3-Fl. (*B*) Germination of GA biosynthesis mutant *ga1* treated with GA_3-Fl, Fl, or GA_3 (100 μM). (*C* and *D*) Hypocotyl elongation of seedlings treated with Paclo (2 μM) plus GA_3-Fl, Fl, or GA_3 (10 μM). Shown are averages ± SE (n = 10). (*D*) Graphical representation of the experiment in *C*. (Scale bar, 1 mm.) (*E*) Root elongation of seedlings treated with Paclo and GA_3-Fl, Fl, or GA_3 (10 μM). Shown are averages ± SE (n = 10). (*F*) Response of Paclo-treated seedlings to increasing concentrations of GA_3 and GA_3-Fl (molecule **3**). EC_{50} is for GA_3 and GA_3-Fl. Shown are averages ± SE (n = 10). (*G*) Molecular structure of GA_4 labeled with Fl. (*H*) Effects of Paclo (2 μM) and GA_4-Fl or GA_4 (10 μM) on germination of WT seeds. Shown are averages ± SE (n = 70). (*I* and *J*) Fluorescence HPLC chromatograms of root extracts from GA_3-Fl–treated (*I*) or GA_4-Fl–treated (*J*) plants and reference compounds. Green, reference molecule; blue, 1-d root extract; yellow, 2-d root extract; red, 3-d root extract. (*I*) Peaks 1 and 2 elute similarly to the GA_3-Fl isomer reference and were further identified by HRMS. (*J*) Peak 1 elutes similarly to GA_4-Fl reference and was further identified by HRMS. Peak 2 is an unidentified GA_4-Fl adduct. Arrows point to retention times expected for GA_3-Fl and GA_4-Fl cleavage products: blue: C6 amide, black: 5- and 6-carboxyfluorescein (*SI Appendix*, Fig. S10*E*). *Significantly different relative to respective Paclo treatment at $P \leq 0.001$ by Student t test.

GA-Fls Interact with the GA Receptors and Are Not Significantly Metabolized in Vivo. GA metabolism in plants is highly complex, and most of the metabolites are biologically inactive (8). To test whether the observed bioactivity of the tagged GAs is due to the intact molecules and not degradation products or secondary metabolites, we first studied their activity in vitro. GA response is initiated by the binding of GAs to the GID1 receptor to promote its association with repressors of GA response called DELLA proteins. This association triggers degradation of the DELLAs via the $SCF^{SLY2/SNE}$ ubiquitin E3 ligase and activation of GA responses (12, 26). To test for interaction between GA-Fl and the receptor, GST-GID1b was expressed in *Escherichia coli* and incubated with Myc-RGA [Repressor of GA, synthesized in TnT (Promega)] in the presence or absence of the tagged GAs. GA_3-Fl and GA_4-Fl promoted interaction between GID1b and the DELLA protein, whereas molecule **1**, which was biologically inactive in vivo, did not promote this interaction (*SI Appendix*, Fig. S9*A*). Similarly, in the yeast two-hybrid system, GA_3-Fl and GA_4-Fl enhanced the interaction between GID1a and RGA (*SI Appendix*, Fig. S9*B*). In both pull-down and yeast two-hybrid assays, GA_4-Fl showed a higher activity compared with GA_3-Fl.

Next, we evaluated the stability of the tagged GAs in plants. For this, extracts from plants treated with either GA_3-Fl or GA_4-Fl for up to 3 d (same conditions as used in bioactivity assays) were prepared and analyzed by HPLC-HRMS (high resolution mass spectrometry). The fluorescence HPLC chromatograms of GA_3-Fl–treated roots (Fig. 1*I*) show two major fluorescent components in the extracts (peaks 1 and 2 in Fig. 1*I*) with no buildup of other fluorescent components over time. Peaks 1 and 2 eluted similarly to the two GA_3-Fl isomers (synthesized from 5- and 6-carboxyfluorescein, peaks 2 and 1, respectively) and were further identified by HRMS [calculated for GA_3-Fl $(M+H^+)$: 835.3073; found: 835.3071 and 835.3066, peaks 1 and 2, respectively (*SI Appendix*, Fig. S10*A*)]. In the GA_4-Fl extracts (GA_4-Fl was synthesized from the single 5-carboxyfluorescein isomer) (Fig. 1*J*), the major fluorescent component (peak 1) is intact GA_4-Fl [calculated for GA_4-Fl $(M+H^+)$: 821.3280; found: 821.3293], yet an additional fluorescent component that increased over time with a molecular mass of 1,308 Da was detected (peak 2) (*SI Appendix*, Fig. S10*B*). The higher molecular mass of this substance (+488 Da, compared with GA_4-Fl) suggests that it is an adduct of GA_4-Fl. However, its molecular identity was not determined. Interestingly, formation of the GA_4-Fl metabolite was observed in root but not in shoot extracts, whereas in GA_3-Fl extracts there was no difference in the fluorescent content of root and shoot (*SI Appendix*, Fig. S10 *C* and *D*). It is important to note that no cleavage products of the tagged GA's C6 amide or any other degradation products were detected (*SI Appendix*, Fig. S10*E*). Altogether, these results establish that the bioactivity of GA_3-Fl and GA_4-Fl arises from the intact molecules and demonstrate their in vivo stability. Because GA_3-Fl proved more resistant to in vivo metabolism, it was preferred for use in further studies.

GA_3-Fl and GA_4-Fl Accumulate to High Levels in Endodermal Cells of the Root Elongation Zone. Roots exhibit an apical-basal developmental gradient starting at the rootward end with the stem cell population in the root meristem. Upon emergence from the stem cell niche, cells undergo multiple rounds of cell division. As cells move farther shootward, they begin to mature and enter the elongation zone. About 6 h later, when they reach their final size, the cells become part of the differentiation zone (Fig. 2*A* and *SI Appendix*, Fig. S11) (27, 28). Cell-type–specific expression of a nondegradable form of the GA-signaling protein GAI revealed that inhibition of GA signaling in the endodermal layer had a particularly dramatic effect on root elongation (29). This suggests that these cells have a unique role in GA regulation of root growth. In addition, interaction between the transcriptional regulators SCL3 and the DELLAs plays a role in controlling GA response and biosynthesis in the endodermis (30, 31). To determine whether GA distribution might contribute to this specificity, we studied the distribution of GA_3-Fl in *Arabidopsis* roots. GA_3-Fl or Fl (5 and 0.5 μM, respectively) was applied to 6-d-old seedlings for 2 h by adding the compound to agar growth medium. Roots were comprehensively washed and immediately imaged. Interestingly, although Fl could be detected uniformly in all tissues (Fig. 2 *C* and *D*), GA_3-Fl was distributed in a highly specific pattern (Fig. 2 *B*–*D*), accumulating in the endodermal cells of the elongation zone (Fig. 2 *B*–*E*). Although GA_3-Fl was applied evenly to the whole root, very low levels could be

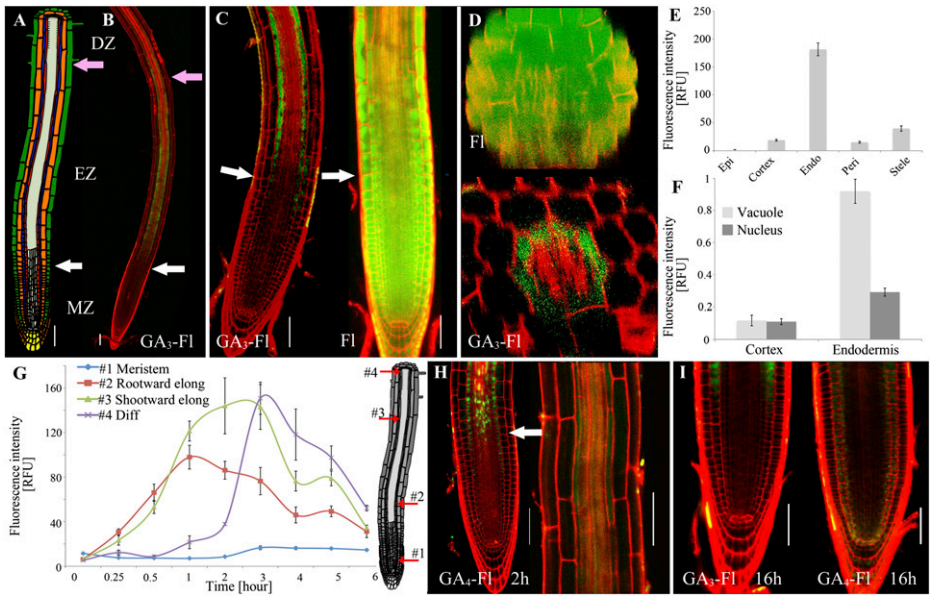

Fig. 2. Distribution of GA_3-Fl and GA_4-Fl in the root. (*A*) Tissue organization and developmental zones of the *Arabidopsis* primary root. MZ, meristematic zone; EZ, elongation zone; DZ, differentiation zone. Green, epidermis; orange, cortex; purple, endodermis; red, pericycle. See *SI Appendix*, Fig. S11, for high-resolution image. (*B*) Confocal image of fluorescence distribution in elongating endodermal cells of roots treated with GA_3-Fl (green) (5 μM, 2 h). White arrows mark transition from MZ to EZ; pink arrow marks transition from EZ to DZ. Cell walls were stained with propidium iodide (red). (*C*) Fl and GA_3-Fl distribution at the transition between meristematic and elongation zones. White arrows mark transition from MZ to EZ (cortical cell is twice the size of shootward previous cell). (*D*) Fl and GA_3-Fl distribution in radial confocal sections of the elongation zone. GA_3-Fl accumulates in the endodermal cells. (*E*) Quantification of GA_3-Fl fluorescence intensity in different cell types of the root elongation zone. Shown are averages ± SE (3 root images, 10 cells/image, 2 sampling points/cell; $n = 60$). RFU, relative fluorescence units. (*F*) Quantification of GA_3-Fl fluorescence intensity in the vacuole and nucleus of cortical and endodermal cells of the elongation zone. Fluorescence intensity was normalized relative to nuclear marker *35S:H2B-RFP*. Shown are averages ± SE (three root images, three cells/image, three sampling points/cell; $n = 27$) (*SI Appendix*, Fig. S16). (*G*) Time-lapse quantification of GA_3-Fl fluorescence intensity in endodermal cells at four different maturation points by confocal imaging. Point 1, meristematic; 2, rootward elongation; 3, shootward elongation; 4, rootward differentiation cells. Shown are averages ± SE (3 root images, 10 cells/image, 2 sampling points/cell; $n = 60$). (*H*) Distribution of GA_4-Fl (5 μM, 2 h) in the root. White arrow marks transition from MZ to EZ. Image on the right is a magnification of the elongation zone. (*I*) Distribution of GA_3-Fl or GA_4-Fl (5 μM) in the root after application for 16 h. (Scale bars, 50 μm.)

detected in the meristematic or differentiation zones (Fig. 2 *B* and *G*). It is important to note that fluorescence intensity of Fl-treated roots was dramatically higher (~22-fold) than for GA_3-Fl–treated roots (*SI Appendix*, Fig. S12). Remarkably, the boundaries of accumulation corresponded precisely to the transition zones from meristematic to elongating cells and from elongating to differentiating cells (*SI Appendix*, Fig. S13).

It is unlikely that the Casparian strip is responsible for the observed pattern as this structure is established shootward to the region of GA_3-Fl accumulation (32). Nevertheless, we examined GA_3-Fl distribution in the *casp1-1 casp3-1* double mutant (33) and in WT plants treated with piperonylic acid, an inhibitor of monolingnol biosynthesis that blocks Casparian strip formation in newly forming cells (34). In both cases, the pattern of GA_3-Fl distribution was unaffected compared with WT plants (*SI Appendix*, Fig. S14), confirming that the Casparian strip does not determine GA_3-Fl accumulation in these cells.

Time-lapse confocal microscopy revealed a dynamic uptake process where GA_3-Fl begins to accumulate within 15 min in the endodermis (Fig. 2*G*). Interestingly, a strong reduction of GA_3-Fl signal could be detected 4 h after application (Fig. 2*G* and *SI Appendix*, Fig. S15).

Subcellular imaging of the elongating endodermal cells showed that GA_3-Fl accumulates mainly in the vacuole and to a lesser extent in the nucleus (Fig. 2*F* and *SI Appendix*, Fig. S16). Importantly, the fluorescent signal in the nuclei of elongating cells was higher in endodermal cells than in other cell types. It should be noted that, in the acidic environment of vacuoles (pH ~5.5), the fluorescence intensity of the Fl-labeled GAs would be decreased (fluorescein's pK: ~6.4); thus, the effective concentration difference between vacuole and nucleus is probably higher than that observed by fluorescence intensity ratio.

GA_4-Fl was distributed in the developing root similarly to GA_3-Fl with high levels of accumulation in the elongating endodermal cells, but was also detectable in the stele after 2 h of application (Fig. 2*H*). Examination of lateral roots showed that here, as well, GA_4-Fl accumulates mostly in the elongating cells of the endodermis (*SI Appendix*, Fig. S17). Additionally, GA_4-Fl accumulation was greatest in the endodermal cell of the main root opposite to the site of lateral root formation. Application of the tagged GAs for longer periods (16 h) resulted in additional accumulation in the transition zone from elongating to meristematic zones, and, for GA_4-Fl, very low levels were also detectable in the meristem's cortex (Fig. 2*I*). The detection of GA_4-Fl in the ground tissues is in accordance with previous findings that GA signaling in ground tissue affects meristem size (35).

GA Marker GFP-RGA Shows Weaker Signal in the Elongating Endodermal Cells. The specific distribution in the root observed for the tagged GAs prompted us to independently evaluate endogenous GA levels. To do this, we examined the expression of the DELLA reporter GFP-RGA in developing roots of *pRGA:GFP-RGA* transgenic plants. GFP-RGA is degraded in the presence of GA through the action of the E3 ligase $SCF^{SLY2/SNE}$ (36, 37). Strikingly, GFP-RGA distribution is complementary to that of the tagged GA in both the meristematic and the elongation zones (Fig. 3*A*). In the presence of Paclo, when endogenous GA synthesis is inhibited, GFP-RGA signal was detected at high levels in the nuclei of all cells in the elongation zone (Fig. 3 *B* and *C*). In the absence of Paclo, although modest reduction in the GFP-RGA signal was observed in all cell types of the elongation zone (0.4-fold reduction in cortex cells), the most substantial drop was observed in the endodermis (17.2-fold reduction) (Fig. 3 *B* and *D*), indicating that endogenous GA level in the endodermis cells is higher than in other cell layers of the elongation zone.

GA_3-Fl Accumulation in Roots Is Actively Regulated. The preferential accumulation of GA in elongating endodermal cells could be due to an active transport or a diffusive process. To address this question, we first evaluated the effect of unlabeled GA_3 on GA_3-Fl distribution. Cotreatment with GA_3-Fl and increasing concentrations of GA_3 led to a decreased fluorescence signal in the elongating endodermal cells and was completely blocked at 20-fold GA_3 excess (Fig. 4*A* and *SI Appendix*, Fig. S18). In contrast, no effect was observed on Fl signal intensity or distribution. We next examined the effect of temperature on GA_3-Fl distribution. In Fl-treated plants maintained at low temperature (4 °C), fluorescence intensity in the roots was relatively high (Fig. 4 *D* and *F*) and was reduced threefold compared with normal growth conditions (22 °C) (Fig. 4*G* and *SI Appendix*, Fig. S19). In

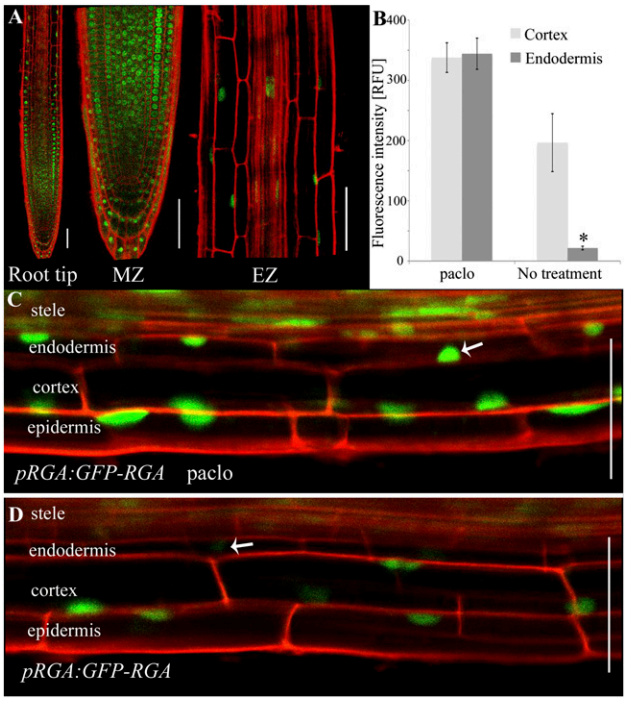

Fig. 3. GFP-RGA signal is reduced in elongating endodermal cells. (*A*) GFP-RGA localization in the root. MZ, meristematic zone; EZ, elongation zone. (*B*) Relative fluorescence intensity of GFP-RGA in the cortex and endodermal nuclei of the elongation zone with and without 2 M Paclo treatment. Shown are averages ± SE (three root images, three cells/image, three sampling points/cell; $n = 27$). (*C* and *D*) Images of the elongation zone showing GFP-RGA levels (*C*) with (*D*) without Paclo treatment. White arrows indicate the endodermal cell nuclei. *Significantly different relative to the respective cortex cell at $P \leq 0.001$ by Student t test. (Scale bars, 50 μm.)

contrast, exposure to lower temperature (4 °C) had a marked effect on GA_3-Fl distribution (40-fold reduction in fluorescence intensity compared with 22 °C), effectively inhibiting its accumulation (Fig. 4 *D*–*G*) and suggesting that the GA transport machinery is energy-dependent. To further test this possibility, GA_3-Fl and Fl accumulation were examined following a 2-h application of three mitochondrial ATP synthesis inhibitors: antimycin A, oligomycin A, and myxothiazol. Whereas Fl accumulation was unaffected by antimycin A and oligomycin A and elevated by myxothiazol, GA_3-Fl uptake was reduced approximately fivefold by all three ATP synthesis inhibitors (Fig. 4*H* and *SI Appendix*, Fig. S20).

To further understand the role of the endodermal cell type in GA accumulation, we tested GA_3-Fl distribution in *scarecrow* (*scr*) and *short-root* (*shr*) mutants. Both SCR and SHR are involved in specification of the ground tissue cell layers, the endodermis and cortex. In the *scr-3* mutant, the ground tissue consists of a single layer of cells with attributes of both cortex and endodermis (38). The *shr-2* mutant also has a single layer of ground tissue, but in this case the cells are cortical in nature (39, 40). GA_3-Fl application to the *scr-3* mutant resulted in strong accumulation in the single layer of ground tissue (Fig. 4*C*). In contrast, no accumulation was observed in the ground tissue of *shr-2* (Fig. 4*C*), indicating that the elongating endodermal cells have unique features that drive GA accumulation. Collectively, these results indicate that GA_3-Fl uptake is an active and saturable process that results in regulated accumulation in the endodermis of the elongation zone.

Ethylene Inhibits GA Accumulation in the Root. The plant hormone ethylene has an important role in the regulation of root development (41–43). Application of ethylene to seedlings results in rapid inhibition of root elongation (44). Studies have shown that ethylene acts, in part, by stabilizing the DELLA proteins (45–47). The involvement of ethylene in GA signaling prompted us to explore its effect on GA distribution. Thus, seedlings were treated with the immediate precursor of ethylene, 1-aminocyclopropane-1-carboxylic (ACC) (48), for 2 h and transferred to medium with ACC and GA_3-Fl. Endodermal accumulation of GA_3-Fl was dramatically inhibited by ACC (Fig. 5 *A* and *B*). To determine if the canonical ethylene-signaling pathway regulates this response, we used *constitutive triple response1-1* (*ctr1-1*), a mutation in a negative regulator of ethylene signaling, and the *ethylene insensitive2-5* (*ein2-5*), a mutation in a key positive regulator of ethylene signaling (43). As expected, GA_3-Fl did not accumulate in the endodermis of *ctr1-1* roots whereas accumulation was observed in *ein2-5* roots in both the presence and the absence of ACC (Fig. 5 *C* and *D*). Coapplication of ACC and Paclo also inhibited GA_3-Fl uptake, implying that ACC does not affect GA_3-Fl accumulation by activating endogenous GA biosynthesis that leads to competition (*SI Appendix*, Fig. S21). Because roots exposed to ACC for 4 h and roots of the *ctr1-1* mutant display developmental changes, including impaired elongation (44), the alteration in GA_3-Fl distribution could be a secondary effect. To clarify this, ACC and GA_3-Fl were applied simultaneously to seedlings roots and imaged after 1 h. Under these conditions, GA_3-Fl accumulation in the elongating endodermal cells was dramatically inhibited in the ACC-treated roots compared with the no-ACC treatment control (*SI Appendix*, Fig. S21), confirming that ethylene is responsible for the observed GA accumulation inhibition. Altogether, these results demonstrate that ethylene signaling affects GA distribution, suggesting that ethylene regulation of GA signaling in *Arabidopsis* roots may be mediated, at least part, through changes in GA transport.

Discussion

Our studies demonstrate the value of fluorescent labeling of plant hormones to study dynamic processes involved in hormone localization and regulation. Recently, Irani et al. fluorescently labeled brassinosteroid (BR) to study BR receptor endocytosis during signaling (49).

Here, we use fluorescently labeled GAs to reveal the distribution of GA in *Arabidopsis* roots. We show that GA accumulates specifically in the endodermis of the root elongation zone. Our results suggest that the endodermis has a special role in GA regulation, consistent with previous studies that indicate that the endodermis is the major GA-responsive tissue in the root (29–31, 35).

Previous studies indicate that the expression of GA biosynthetic genes is particularly high in the meristem with lower levels in other cell types (50–53). Our observation that the labeled GAs accumulate in elongating endodermal cells suggests that GA synthesized in the meristem, as well as in the cortical and epidermal cell layers, moves to the endodermis where it regulates elongation growth. Cells enter the elongation zone for a short period where they increase their length by ~10-fold over 5 h. This size increase would result in a corresponding rapid intracellular dilution of GA levels unless new GA is either synthesized in the endodermis or transported from surrounding tissues (52).

We observe a striking accumulation of GA in the vacuoles of endodermal cells. Vacuolar accumulation may act to buffer GA levels within these cells, thus controlling GA concentration in the cytoplasm and nucleus where the hormone is thought to act. The observation that both fluorescent and native GA are present at a higher level in the nuclei of elongating endodermal cells compared with other cell types supports this notion. In a similar way, the decrease in GA_3-Fl accumulation in elongating endodermis that was observed after 4 h (Fig. 2*G*) may reflect feedback inhibition of GA uptake. According to this model, new endodermal cells that form after several hours of treatment would accumulate less GA.

It is important to note that our results do not address the specificity of the suggested transport machinery. Thus, it is possible that this machinery transports additional plant hormones or other small molecules. Consistent with this possibility, a recent study

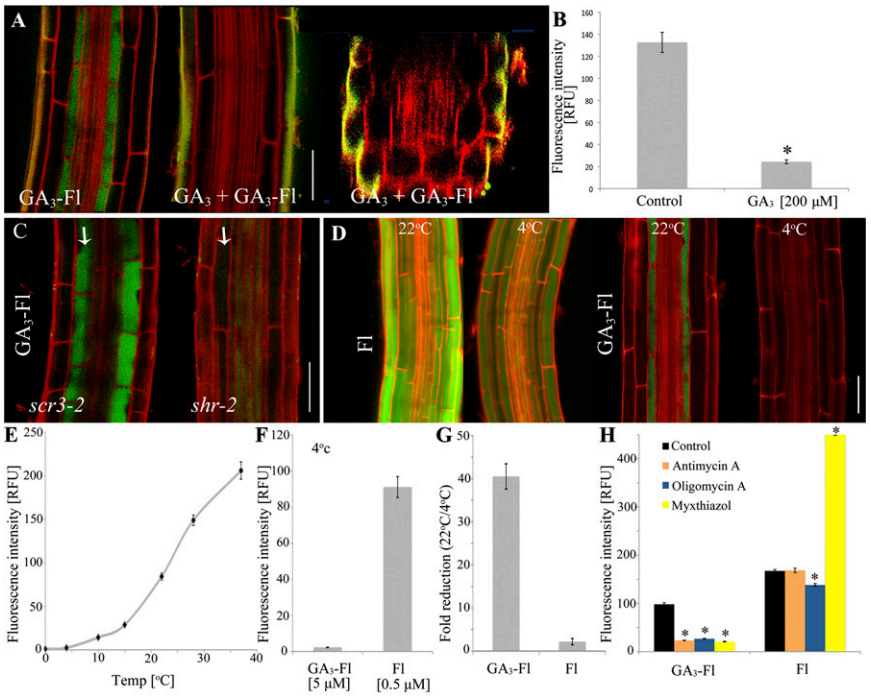

Fig. 4. GA_3-Fl is actively transported into the elongating endodermal cells. (*A*) Distribution of GA_3-Fl (5 μM) in the root elongation zone in the absence or presence of competing GA_3 (200 μM). At the far right is a radial confocal section of the elongation zone under competing conditions (compare with Fig 2*D*). (*B*) Quantification of the competition assay described in *A*. Fluorescence intensity was measured in the elongating endodermal cells. Shown are averages ± SE (3 root images, 10 cells/image, 2 sampling points/cell; n = 60) (*SI Appendix*, Fig. S18). (*C*) GA_3-Fl distribution in the elongation zone of the *scr3-2* and *shr-2* mutants. White arrows indicate the single cortex/endodermal layer. (*D*) Temperature dependence of Fl and GA_3-Fl accumulation in the elongation zone. Fl (0.5 μM) and GA_3-Fl (5 μM) were applied for 2 h at either 4 °C or 22 °C. (*E*) Fluorescence intensity in elongating endodermal cells in plants treated with GA_3-Fl (5 μM) for 2 h at the indicated temperature. Shown are averages ± SE (n = 60). (*F*) Fl and GA_3-Fl applied for 2 h at 4 °C. Fluorescent intensity was measured as described in *B*. (*G*) Fold change in fluorescence intensity of Fl (0.5 μM) and GA_3-Fl (5 μM) applied to seedlings exposed to 4 °C compared with 22 °C. Fluorescence intensity was measured as described in *B*. (*H*) ATP synthesis inhibitors antimycin A, oligomycin A, and myxothiazol disrupt GA_3-Fl but not Fl accumulation in the elongation zone. Seedlings were treated with 10 μM of the indicated inhibitor for 1.5 h and transferred to plates with inhibitor + GA_3-Fl or Fl (5 μM and 0.5 μM, respectively) for an additional 1.5 h. Fluorescence intensity was measured in the elongating endodermal cells. Shown are averages ± SE (n = 60). *Significantly different relative to the respective control at $P \leq 0.001$ by Student t test. (Scale bars, 50 μm.)

demonstrated that AIT3, a member of the NRT1/PTR family, can transport abscisic acid (ABA) as well as GA_3 in yeast (6). At present, the mechanism of GA accumulation in the endodermis is unclear, but the fluorescent GAs can be used in combination with genetic screening to identify proteins involved in this process. In addition, introduction of a photo-crosslinking moiety into the fluorescent GA structure may facilitate the isolation of such proteins.

Physiological studies have revealed complex interactions between all of the major plant hormones during root development. The discovery that ethylene regulates GA distribution introduces an additional dimension to this complex picture. Based on our results, ethylene may regulate root growth in part by affecting the level of GA in the endodermis. Because ethylene was shown to regulate auxin transport and biosynthesis in the root elongation zone (54), it would be interesting to test whether ethylene's effect on GA distribution is mediated by auxin. Dynamic regulation of GA levels by ethylene and perhaps other hormones may contribute to environmental regulation of root growth.

GAs regulate diverse processes throughout plant growth and development. It is likely that GA distribution, regulated by localized synthesis, transport, and inactivation, will be an important aspect of GA action in various plant tissues. For example, GA transport was recently shown to be involved in xylem expansion (6). We expect that the labeled GAs that we describe here will help to dissect this and other GA-regulated processes.

Unraveling the molecular details of plant hormone transport mechanisms will contribute to a more comprehensive understanding of hormone action. Our study emphasizes the significance of plant hormone mapping, demonstrating that fluorescent labeling is a compelling tool to understand spatial and temporal distribution of hormones and other small signaling molecules.

Methods Summary

Chemical Synthesis and Characterization. Synthetic schemes, procedures, and compound characterization are reported in *SI Appendix*.

Bioactivity Assays. For germination bioactivity assay with the GA biosynthesis mutant *ga1-1*, seeds were placed in liquid (100 μM) with the indicated treatments for 2 d at 4 °C and transferred to the dark at 22 °C for 2 more days. Subsequently, the seeds were plated on vertical MS plates, and germination was scored under a dissecting scope 3 d later. For germination assays with Paclo, seeds were placed on vertical plates with 2 μM Paclo and 10 μM of molecules **1**–**4**, Fl, or GA_3. Germination was scored under a dissecting scope 5 d later. For root growth dose–response assays (Fig. 1*F* and *SI Appendix*, Fig. S7), 5-d-old seedlings were transferred onto fresh MS media with either GA_3 or GA_3-Fl for 7 additional days after which root length was measured. Root growth in Fig. 1*E* was performed in a similar way except the

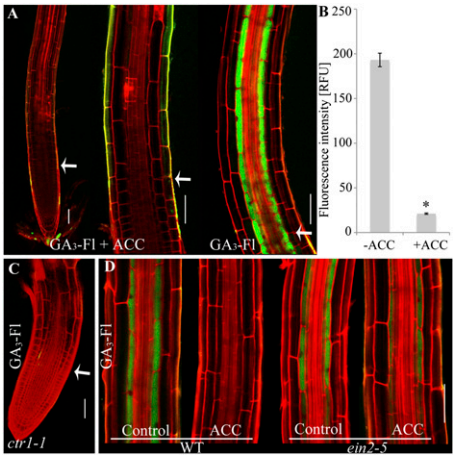

Fig. 5. Ethylene inhibits GA accumulation in the root. (*A*) Effect of ACC treatment on GA_3-Fl distribution in the elongation zone. Seedlings were treated with 1 μM ACC for 1.5 h, transferred to ACC + GA_3-Fl (1 μM + 5 μM, respectively), and imaged 1.5 h later. Center image is a magnification of the elongation zone. Right image is a control (GA_3-Fl distribution in the root elongation zone treated with GA_3-Fl for 1.5 h and imaged at the same conditions and settings). (*B*) Graphical representation of the experiment in *A*. Shown are averages ± SE (three root images, 10 cells/image, two sampling points/cell; n = 60) (*C*) GA_3-Fl distribution in *ctr1-1* mutant. (*D*) GA_3-Fl distribution in *ein2-5* mutant and WT (control) with and without 1 μM ACC. *Significantly different relative to control at $P \leq 0.001$ by Student t test. (Scale bars, 50 μm.)

seedlings were transferred at day 4, and root growth was measured after a further 5 d. For hypocotyl assays, seedlings were transferred at day 4 and measured 5 d later. Ten-day-old tomato seedlings were treated three times a week for 2 wk (shoot apical meristem and small leaves) with liquid solution of 10 μM of the indicated compounds. The mature third leaf was imaged. Seed germination and root and hypocotyl growth were all imaged and measured using a Nikon SMZ1500 dissecting scope and ImageJ software (http://rsbweb.nih.gov/ij/index.html).

Complete methods are described in *SI Appendix*.

ACKNOWLEDGMENTS. We thank Larry Gross (University of California at San Diego) for mass spectroscopy; Joseph Ecker (The Salk Institute for Biological Studies) for sharing *ein2-5* and *ctr1-1* mutants; the Arabidopsis Biological Research Center (ABRC) (The Ohio State University), which provided *Arabidopsis pRGA:GFP-RGA*, *shr-2*, and *scr-3* lines; and Tai-ping Sun for the pull-down pGEX-GID1b (GST-GID1b) plasmid and the yeast two-hybrid DB-GID1a/AD-RGA plasmids. This work was funded by Vaadia–BARD Postdoctoral Fellowship FI-431-10 (to E.S.); a Machiah Foundation/Jewish Community Federation Fellowship (E.S.); R25T CRIN Training Grant 5R25CA153915-03 (to R.W.); The Marc and Eva Stern Foundation (E.K.); Human Frontier Science Program (HFSP) Fellowship LT000159/2009-L (to E.K.); National Science Foundation Grant IOS10-45256 (to J.C.); National Institutes of Health Grants 1R01 GM094428 (to J.C.), NS27177 (to R.Y.T.), and 1R01 GM43644 (to M.E.); Department of Energy Grant DE-FG02-11ER16007 (to M.E.); the Howard Hughes Medical Institute (J.C., R.Y.T., and M.E.); and the Gordon and Betty Moore Foundation (M.E.).

1. Wolters H, Jürgens G (2009) Survival of the flexible: Hormonal growth control and adaptation in plant development. *Nat Rev Genet* 10(5):305–317.
2. Blilou I, et al. (2005) The PIN auxin efflux facilitator network controls growth and patterning in Arabidopsis roots. *Nature* 433(7021):39–44.
3. Vanneste S, Friml J (2009) Auxin: A trigger for change in plant development. *Cell* 136(6):1005–1016.
4. Kretzschmar T, et al. (2012) A petunia ABC protein controls strigolactone-dependent symbiotic signalling and branching. *Nature* 483(7389):341–344.
5. Kuromori T, et al. (2010) ABC transporter AtABCG25 is involved in abscisic acid transport and responses. *Proc Natl Acad Sci USA* 107(5):2361–2366.
6. Kanno Y, et al. (2012) Identification of an abscisic acid transporter by functional screening using the receptor complex as a sensor. *Proc Natl Acad Sci USA* 109(24):9653–9658.
7. Fleet CM, Sun TP (2005) A DELLAcate balance: The role of gibberellin in plant morphogenesis. *Curr Opin Plant Biol* 8(1):77–85.
8. Yamaguchi S (2008) Gibberellin metabolism and its regulation. *Annu Rev Plant Biol* 59:225–251.
9. Brian PW (1959) Effects of gibbrellins on plant growth and development. *Biol Rev Camb Philos Soc* 34(1):37–84.
10. Shimada A, et al. (2008) Structural basis for gibberellin recognition by its receptor GID1. *Nature* 456(7221):520–523.
11. Murase K, Hirano Y, Sun TP, Hakoshima T (2008) Gibberellin-induced DELLA recognition by the gibberellin receptor GID1. *Nature* 456(7221):459–463.
12. Ueguchi-Tanaka M, et al. (2005) GIBBERELLIN INSENSITIVE DWARF1 encodes a soluble receptor for gibberellin. *Nature* 437(7059):693–698.
13. Peng J, et al. (1999) 'Green revolution' genes encode mutant gibberellin response modulators. *Nature* 400(6741):256–261.
14. Middleton AM, et al. (2012) Mathematical modeling elucidates the role of transcriptional feedback in gibberellin signaling. *Proc Natl Acad Sci USA* 109(19):7571–7576.
15. Ragni L, et al. (2011) Mobile gibberellin directly stimulates Arabidopsis hypocotyl xylem expansion. *Plant Cell* 23(4):1322–1336.
16. Eriksson S, Böhlenius H, Moritz T, Nilsson O (2006) GA4 is the active gibberellin in the regulation of LEAFY transcription and Arabidopsis floral initiation. *Plant Cell* 18(9):2172–2181.
17. Dayan J, et al. (2012) Leaf-induced gibberellin signaling is essential for internode elongation, cambial activity, and fiber differentiation in tobacco stems. *Plant Cell* 24(1):66–79.
18. Hu J, et al. (2008) Potential sites of bioactive gibberellin production during reproductive growth in Arabidopsis. *Plant Cell* 20(2):320–336.
19. Liebisch HW, Bene ŠJ, Bene ŠI (1988) Comparative investigations on the metabolic fate of a GA3 amino acid conjugate with those of glucosides and derivatives of GA3. *Biol Plant* 30(2):120–123.
20. Kahn A, Goss JA, Smith DE (1957) Effect of Gibberellin on germination of lettuce seed. *Science* 125(3249):645–646.
21. Ogawa M, et al. (2003) Gibberellin biosynthesis and response during Arabidopsis seed germination. *Plant Cell* 15(7):1591–1604.
22. Koornneef M, Veen JH (1980) Induction and analysis of gibberellin sensitive mutants in *Arabidopsis thaliana* (L.) Heynh. *Theor Appl Genet* 58(6):257–263.
23. Sun TP, Kamiya Y (1994) The Arabidopsis GA1 locus encodes the cyclase ent-kaurene synthetase A of gibberellin biosynthesis. *Plant Cell* 6(10):1509–1518.
24. de Lucas M, et al. (2008) A molecular framework for light and gibberellin control of cell elongation. *Nature* 451(7177):480–484.
25. Frankland B, Wareing PF (1960) Effect of gibberellic acid on hypocotyl growth of lettuce seedlings. *Nature* 185(4708):255–256.
26. Griffiths J, et al. (2006) Genetic characterization and functional analysis of the GID1 gibberellin receptors in Arabidopsis. *Plant Cell* 18(12):3399–3414.
27. Ubeda-Tomás S, Beemster GT, Bennett MJ (2012) Hormonal regulation of root growth: Integrating local activities into global behaviour. *Trends Plant Sci* 17(6):326–331.
28. Petricka JJ, Winter CM, Benfey PN (2012) Control of Arabidopsis root development. *Annu Rev Plant Biol* 63:563–590.
29. Ubeda-Tomás S, et al. (2008) Root growth in Arabidopsis requires gibberellin/DELLA signalling in the endodermis. *Nat Cell Biol* 10(5):625–628.
30. Heo JO, et al. (2011) Funneling of gibberellin signaling by the GRAS transcription regulator scarecrow-like 3 in the Arabidopsis root. *Proc Natl Acad Sci USA* 108(5):2166–2171.
31. Zhang ZL, et al. (2011) Scarecrow-like 3 promotes gibberellin signaling by antagonizing master growth repressor DELLA in Arabidopsis. *Proc Natl Acad Sci USA* 108(5):2160–2165.
32. Alassimone J, Naseer S, Geldner N (2010) A developmental framework for endodermal differentiation and polarity. *Proc Natl Acad Sci USA* 107(11):5214–5219.
33. Roppolo D, et al. (2011) A novel protein family mediates Casparian strip formation in the endodermis. *Nature* 473(7347):380–383.
34. Naseer S, et al. (2012) Casparian strip diffusion barrier in Arabidopsis is made of a lignin polymer without suberin. *Proc Natl Acad Sci USA* 109(25):10101–10106.
35. Ubeda-Tomás S, et al. (2009) Gibberellin signaling in the endodermis controls Arabidopsis root meristem size. *Curr Biol* 19(14):1194–1199.
36. Achard P, et al. (2006) Integration of plant responses to environmentally activated phytohormonal signals. *Science* 311(5757):91–94.
37. Silverstone AL, et al. (2001) Repressing a repressor: Gibberellin-induced rapid reduction of the RGA protein in Arabidopsis. *Plant Cell* 13(7):1555–1566.
38. Di Laurenzio L, et al. (1996) The SCARECROW gene regulates an asymmetric cell division that is essential for generating the radial organization of the Arabidopsis root. *Cell* 86(3):423–433.
39. Benfey PN, et al. (1993) Root development in Arabidopsis: Four mutants with dramatically altered root morphogenesis. *Development* 119(1):57–70.
40. Helariutta Y, et al. (2000) The SHORT-ROOT gene controls radial patterning of the Arabidopsis root through radial signaling. *Cell* 101(5):555–567.
41. Smith KA, Robertson PD (1971) Effect of ethylene on root extension of cereals. *Nature* 234(5325):148–149.
42. Swarup R, et al. (2007) Ethylene upregulates auxin biosynthesis in Arabidopsis seedlings to enhance inhibition of root cell elongation. *Plant Cell* 19(7):2186–2196.
43. Stepanova AN, Alonso JM (2009) Ethylene signaling and response: Where different regulatory modules meet. *Curr Opin Plant Biol* 12(5):548–555.
44. Le J, Vandenbussche F, Van Der Straeten D, Verbelen JP (2001) In the early response of Arabidopsis roots to ethylene, cell elongation is up- and down-regulated and uncoupled from differentiation. *Plant Physiol* 125(2):519–522.
45. Achard P, Vriezen WH, Van Der Straeten D, Harberd NP (2003) Ethylene regulates Arabidopsis development via the modulation of DELLA protein growth repressor function. *Plant Cell* 15(12):2816–2825.
46. Pierik R, Djakovic-Petrovic T, Keuskamp DH, de Wit M, Voesenek LA (2009) Auxin and ethylene regulate elongation responses to neighbor proximity signals independent of gibberellin and della proteins in Arabidopsis. *Plant Physiol* 149(4):1701–1712.
47. Achard P, et al. (2007) The plant stress hormone ethylene controls floral transition via DELLA-dependent regulation of floral meristem-identity genes. *Proc Natl Acad Sci USA* 104(15):6484–6489.
48. Adams DO, Yang SF (1979) Ethylene biosynthesis: Identification of 1-aminocyclopropane-1-carboxylic acid as an intermediate in the conversion of methionine to ethylene. *Proc Natl Acad Sci USA* 76(1):170–174.
49. Irani NG, et al. (2012) Fluorescent castasterone reveals BRI1 signaling from the plasma membrane. *Nat Chem Biol* 8(6):583–589.
50. Silverstone AL, Chang C, Krol E, Sun TP (1997) Developmental regulation of the gibberellin biosynthetic gene GA1 in Arabidopsis thaliana. *Plant J* 12(1):9–19.
51. Birnbaum K, et al. (2003) A gene expression map of the Arabidopsis root. *Science* 302(5652):1956–1960.
52. Band LR, et al. (2012) Growth-induced hormone dilution can explain the dynamics of plant root cell elongation. *Proc Natl Acad Sci USA* 109(19):7577–7582.
53. Mitchum MG, et al. (2006) Distinct and overlapping roles of two gibberellin 3-oxidases in Arabidopsis development. *Plant J* 45(5):804–818.
54. Růzicka K, et al. (2007) Ethylene regulates root growth through effects on auxin biosynthesis and transport-dependent auxin distribution. *Plant Cell* 19(7):2197–2212.